

Diatomic molecule in a strong infrared laser field: level-shifts and bond-length change due to laser-dressed Morse potential

Sándor Varró^{1,2}, Szabolcs Hack^{1,3,*}, Gábor Paragi^{3,4,5}, Péter Földi^{1,3}, Imre F. Barna², and Attila Czirják^{1,3}

¹ELI ALPS, ELI-HU Non-Profit Ltd., Wolfgang Sandner utca 3., Szeged, H-6728, Hungary

²Wigner Research Centre for Physics, Konkoly Thege Miklós út 29 - 33, H-1121 Budapest, Hungary

³Department of Theoretical Physics, University of Szeged, Tisza L. krt. 84 - 86, H-6720 Szeged, Hungary

⁴Institute of Physics, University of Pécs, Ifjúság útja 6, H-7624 Pécs, Hungary

⁵Department of Medical Chemistry, University of Szeged, Dóm Square 8, H-6720 Szeged, Hungary

* corresponding author: szabolcs.hack@eli-alps.hu

Abstract.

We present a general mathematical procedure to handle interactions described by a Morse potential in the presence of a strong harmonic excitation. We account for permanent and field-induced terms and their gradients in the dipole moment function, and we derive analytic formulae for the bond-length change and for the shifted energy eigenvalues of the vibrations, by using the Kramers-Henneberger frame. We apply these results to the important cases of H₂ and LiH, driven by a near- or mid-infrared laser in the 10¹³ W/cm² intensity range.

Keywords: molecular vibrations, off-resonant excitation, strong-field phenomena, Kramers-Henneberger frame

1. Introduction

Diatomic molecules driven by strong laser pulses show a rich variety of fundamentally important processes, depending on how the laser pulse parameters are related to the diatomic's properties [1, 2, 3]. Strong infrared (IR) pulses, typically in the intensity range of 10¹² – 10¹⁴ W/cm², have gained increasing importance in several recent developments with diatomics. For certain strong-field scenarios, like e.g. gas HHG, mid-IR laser pulses have considerable advantages over near-IR or visible pulses, see the excellent experimental results in [4, 5, 6, 7]. Established pump-and-probe experiments in attosecond and strong-field physics [8] involve a relatively strong IR pulse, like e.g.

in attosecond streaking [9, 10, 11, 12, 13, 14]. An emerging topic in this field of research is molecules in strong IR fields without ionization [15], having obvious relevance also to important experimental techniques of laser manipulation of molecules, like trapping [16], alignment [17], orientation [18]. Ultra-high intensity laser pulses ($10^{18} - 10^{20}$ W/cm²) have a pedestal [19] typically in the intensity range of $10^{10} - 10^{14}$ W/cm² (having also an interesting nontrivial photon statistics [20]) which raises questions and concerns about the true "initial" state of the target molecule when the actual ultra-high intensity pulse reaches it.

Although the theoretical framework for molecules interacting with laser fields is well established [21, 22], analytic results are rare and usually approximate in the strong-field domain, while most of the numerical methods [1, 23, 24, 25] have heavily increasing cost for IR wavelength. Thus, new analytic methods for molecules in strong fields are of great significance.

In this paper, we address the problem of a diatomic molecule driven by a strong IR pulse without ionization. We investigate a scenario where electronic transitions are also avoided, thus the long quasi-monochromatic IR laser pulse affects the nuclear vibrations only, neglecting also the rotational degrees of freedom. Vibrations of a diatomic molecule are well described by the Morse potential [26, 27] which has a large literature from textbooks to current research papers, including a number of modifications and improvements [28, 29, 30]. Some of the recent treatments are based on supersymmetry [31, 32, 33]. Laser driven nuclear dynamics of a diatomic molecule were investigated earlier by many authors, see e.g. [34, 35, 36, 32, 37, 38], however, usually neglecting field-induced terms of the dipole moment function [39, 40, 41]. Due to the moderately strong-field regime we are interested in, we account for permanent and field-induced terms and their gradients in the dipole moment function in the present work. We use atomic units, unless otherwise stated.

2. Theoretical model

The Hamiltonian of a diatomic molecule in center of mass (COM) coordinate system, in the presence of an infrared laser field, treated in dipole approximation and length gauge, is the following:

$$\hat{H} = \hat{H}_0 + \hat{T}_n - \hat{\boldsymbol{\mu}}\mathbf{F}(t), \quad (1)$$

where \hat{H}_0 , the so-called electronic Hamiltonian, contains the electronic kinetic energy operator and the electron-electron, electron-nucleus, nucleus-nucleus potential energy operators and \hat{T}_n is the nuclear kinetic energy operator. In the interaction term $\hat{\boldsymbol{\mu}}$ and $\mathbf{F}(t)$ are the dipole moment operator and the electric field strength, respectively. Assuming laser frequencies that are much smaller than the characteristic frequency of the electronic transitions between ground and excited electronic states (e.g. IR laser fields) we can simultaneously apply the quasistatic approximation to the electronic dynamics and the Born-Oppenheimer (BO) approximation [42]. For any instantaneous value of

the electric field we consider the solution of the time-independent Schrödinger equation (TISE) for the electronic ground state $\phi_0(\mathbf{r}; \mathbf{R}, t)$ to be known:

$$\left[\hat{H}_0 - \hat{\boldsymbol{\mu}} \mathbf{F}(t) \right] \phi_0(\mathbf{r}; \mathbf{R}, t) = \varepsilon_0(\mathbf{R}, F(t)) \phi_0(\mathbf{r}; \mathbf{R}, t), \quad (2)$$

where \mathbf{r} and \mathbf{R} stand for all electronic and for all nuclear coordinates, respectively. Regarding the dynamics of the electronic system, we consider the time and the nuclear coordinates as parameters and we assume that $\hat{\boldsymbol{\mu}}$ and $\mathbf{F}(t)$ are parallel. Thus, instead of \mathbf{R} , we use the internuclear distance R for the diatomic molecule. The field-dependent electronic ground state energy, which plays the role of a potential surface for the nuclear motion, is the sum of two terms:

$$\varepsilon_0(R, F(t)) = \varepsilon_0(R, 0) - \int_0^{F(t)} \mu(R, F') dF', \quad (3)$$

where $\varepsilon_0(R, 0)$ can be approximated by the Morse potential and $\mu(R, F)$ is the dipole moment function which includes the field-free and induced terms.

Applying the BO approximation and projecting the molecular Schrödinger equation onto $\phi_0(\mathbf{r}; R, t)$, the time-dependent Schrödinger equation (TDSE) for the nuclear motion becomes:

$$i\hbar \frac{\partial}{\partial t} \chi(u, t) = \left[-\frac{\hbar^2}{2M_n} \frac{\partial^2}{\partial u^2} + V_M(u) - \int_0^{F(t)} \mu(u, F') dF' \right] \chi(u, t), \quad (4)$$

where $\chi(u, t)$ represent the nuclear wave function, M_n is the reduced nuclear mass, $u = R - R_0$ measures the distance of the two nuclei from its equilibrium value R_0 . The $V_M(u)$ is the Morse potential with the form of

$$V_M(u) = D (e^{-2au} - 2e^{-au}), \quad (5)$$

where $D > 0$ is the potential strength or dissociation energy and a determines the width of the potential well. We take into account the dipole moment function in the following form:

$$\mu(u, F(t)) = \mu_0 + \mu_1 u + \alpha_0 F(t) + \alpha_1 u F(t), \quad (6)$$

where μ_0 and μ_1 are the permanent dipole moment and dipole gradient, α_0 and α_1 are the polarizability and polarizability gradient of the molecule, respectively.

3. Analytic results for level shifts and bond-length change in the case of a monochromatic laser excitation

In the following we assume a long monochromatic laser pulse, i.e. a harmonic excitation $F(t) = F_0 \sin(\omega t)$ with peak electric field strength F_0 and angular frequency ω .

We can easily eliminate the terms containing μ_0 and α_0 in (4) with the following unitary transformation:

$$\chi(u, t) = \exp \left\{ \frac{i}{\hbar} \int_{-\infty}^t \mu_0 F(t') + \alpha_0 F(t')^2 dt' \right\} \varphi_0(u, t), \quad (7)$$

and we get

$$i\hbar\frac{\partial}{\partial t}\varphi_0(u, t) = \left[-\frac{\hbar^2}{2M_n}\frac{\partial^2}{\partial u^2} + V_M(u) + ug(t) - \frac{\alpha_1 F_0^2}{4}u \right] \varphi_0(u, t), \quad (8)$$

where $g(t) = F_0[-\mu_1 \sin(\omega t) + \frac{\alpha_1}{4}F_0 \cos(2\omega t)]$. We apply the next unitary transformation, which is similar to the $\mathbf{p} \cdot \mathbf{A}$ gauge transformation:

$$\varphi_0(u, t) = \exp \left\{ \frac{i}{\hbar} u G(t) \right\} \varphi_1(u, t), \quad \text{where } G(t) = \int_{-\infty}^t g(t') dt'. \quad (9)$$

Then a term with $G(t)^2$ appears in the TDSE, which we eliminate by the unitary transformation $\varphi_1(u, t) = \exp \left\{ \frac{i}{\hbar} \int_{-\infty}^t G^2(t') dt' \right\} \varphi_2(u, t)$. Now the TDSE takes the following form:

$$i\hbar\frac{\partial}{\partial t}\varphi_2(u, t) = \left[\frac{\hat{p}^2}{2M_n} - \frac{\hat{p}}{M_n}G(t) + V_M(u) - \frac{\alpha_1 F_0^2}{4}u \right] \varphi_2(u, t), \quad (10)$$

Within the coordinate range of the bound states, the term $V_M(u) - \frac{\alpha_1 F_0^2}{4}u$ can be very well approximated again by an other Morse potential $\mathcal{V}_M(u)$ having the parameters \tilde{a} and \tilde{D} : by comparing the Taylor series of $V_M(u) - \frac{\alpha_1 F_0^2}{4}u$ to that of $\mathcal{V}_M(u)$ up to the cubic term, the \tilde{a} and \tilde{D} are defined by the following equations:

$$\begin{aligned} 2\tilde{a}^2\tilde{D}\Delta R_0 &= \frac{\alpha_1 F_0^2}{4}, \\ \tilde{a}^2\tilde{D}(1 + 3\tilde{a}\Delta R_0) &= a^2D, \\ \frac{1}{3}\tilde{a}^3\tilde{D}(3 + 7\tilde{a}\Delta R_0) &= a^3D, \end{aligned} \quad (11)$$

where ΔR_0 is the shift of the equilibrium position, i.e. a bond-length change caused by the laser field.

At this point we go over to the so-called Kramers-Henneberger frame [43, 44, 45, 46] with

$$\varphi_2(u, t) = \exp \left\{ \frac{i}{\hbar} \hat{p} \Lambda(t) \right\} \varphi_3(u, t), \quad \text{where } \Lambda(t) = \frac{1}{M_n} \int_{-\infty}^t G(t') dt'. \quad (12)$$

In this frame the potential energy function is shifted by the following oscillating term:

$$\Lambda(t) = c_1 \sin(\omega t) + c_2 \cos(2\omega t), \quad (13)$$

where $c_1 = \mu_1 F_0 / M_n \omega^2$ and $c_2 = \alpha_1 F_0^2 / 16 M_n \omega^2$. The explicit form of the shifted potential with the modified \tilde{D} and \tilde{a} parameters is

$$\mathcal{V}_M(u + \Lambda(t)) = \tilde{D} \left(e^{-2\tilde{a}(u + \Lambda(t))} - e^{-\tilde{a}(u + \Lambda(t))} \right), \quad (14)$$

which contains all of the high-harmonics of the laser field according to series expansions:

$$\begin{aligned} \exp \{ -\tilde{a}c_1 \sin(\omega t) \} &= I_0(\tilde{a}c_1) + 2 \sum_{k=1}^{\infty} I_k(\tilde{a}c_1) \cos[k\omega t + \pi/2], \\ \exp \{ -\tilde{a}c_2 \cos(2\omega t) \} &= I_0(\tilde{a}c_2) + 2 \sum_{k=1}^{\infty} I_k(\tilde{a}c_2) \cos[2k\omega t], \end{aligned} \quad (15)$$

where $I_k(x)$ is the modified Bessel function of the first kind. If the laser frequency sufficiently higher than the vibrational and transition frequencies, then the nuclei "feel" only the time average of the shifted potential over one optical cycle:

$$\langle \mathcal{V}_M(u + \alpha(t)) \rangle = \tilde{D} \left[e^{-2\tilde{a}u} \left(I_0(2\tilde{a}c_1)I_0(2\tilde{a}c_2) + 2 \sum_{k=1}^{\infty} (-1)^k I_{2k}(2\tilde{a}c_1)I_k(2\tilde{a}c_2) \right) - 2e^{-\tilde{a}u} \left(I_0(\tilde{a}c_1)I_0(\tilde{a}c_2) + 2 \sum_{k=1}^{\infty} (-1)^k I_{2k}(\tilde{a}c_1)I_k(\tilde{a}c_2) \right) \right], \quad (16)$$

in which the infinite sums are negligible because the arguments of the modified Bessel functions are very small in the reasonable parameter range. Thus, we get a Morse potential with field modified parameters in Kramers-Henneberger frame [43, 44]:

$$\bar{\mathcal{V}}_M(u) = \langle \mathcal{V}_M(u + \alpha(t)) \rangle = \bar{D} \left(e^{-2\tilde{a}(u-\bar{u}_0)} - 2e^{-\tilde{a}(u-\bar{u}_0)} \right), \quad (17)$$

where

$$\bar{D} \equiv \tilde{D} \frac{I_0^2(\tilde{a}c_1)I_0^2(\tilde{a}c_2)}{I_0(2\tilde{a}c_1)I_0(2\tilde{a}c_2)}, \quad \text{and} \quad \bar{u}_0 \equiv \frac{1}{\tilde{a}} \log \left[\frac{I_0(2\tilde{a}c_1)I_0(2\tilde{a}c_2)}{I_0(\tilde{a}c_1)I_0(\tilde{a}c_2)} \right], \quad (18)$$

are the dissociation energy and the equilibrium position of the Morse potential in the laser field, respectively. Finally, we obtain the energy eigenvalues of (4) as

$$\mathcal{E}_n = -\bar{D} + \hbar\bar{\omega} \left(n + \frac{1}{2} \right) - \frac{\hbar^2\bar{\omega}^2}{4\bar{D}} \left(n + \frac{1}{2} \right)^2, \quad (19)$$

where $\bar{\omega} = \tilde{a} \left(\frac{2\bar{D}}{M_n} \right)^{1/2}$.

4. Vibration level shifts of LiH and H₂

We apply our model to LiH and to H₂ as examples of heteronuclear and homonuclear molecules, respectively. These belong to the most studied diatomic molecules, since both of them have fundamental importance from basic molecular physics to material science and to astrophysics and cosmology [47, 48, 49, 50, 51, 52].

We computed the field-dependent electronic ground state energy $\varepsilon_0(u, F)$ and the molecular dipole moment function $\mu(u, F(t))$ based on density-functional theory (DFT), using the Gaussian 16 program package [53]. The calculation method was selected according to the suggestion of recent benchmark studies [54, 55], where dipole moments for a large test set of molecules, including diatomic molecules were calculated and compared to experimental data. According to the conclusion of Zapata and McKemmish [54], double hybrid functionals (e.g. B3LYP [56]) with quadrupole- ζ -quality basis set [57, 58] is a proper choice for the calculation of small molecules with high accuracy. Figure 1 (a) and (b) present the computed values of $\varepsilon_0(u, 0)$ and it clearly shows that $\varepsilon_0(u, 0)$ can be properly approximated for both molecules in the desired coordinate range by a Morse potential. We present the computed dipole moment function of LiH in figure 2, which is well fitted by (6) in the field strength range from -0.02 to 0.02 a.u. Table 1 contains the numerical values of the relevant parameters for both LiH and H₂.

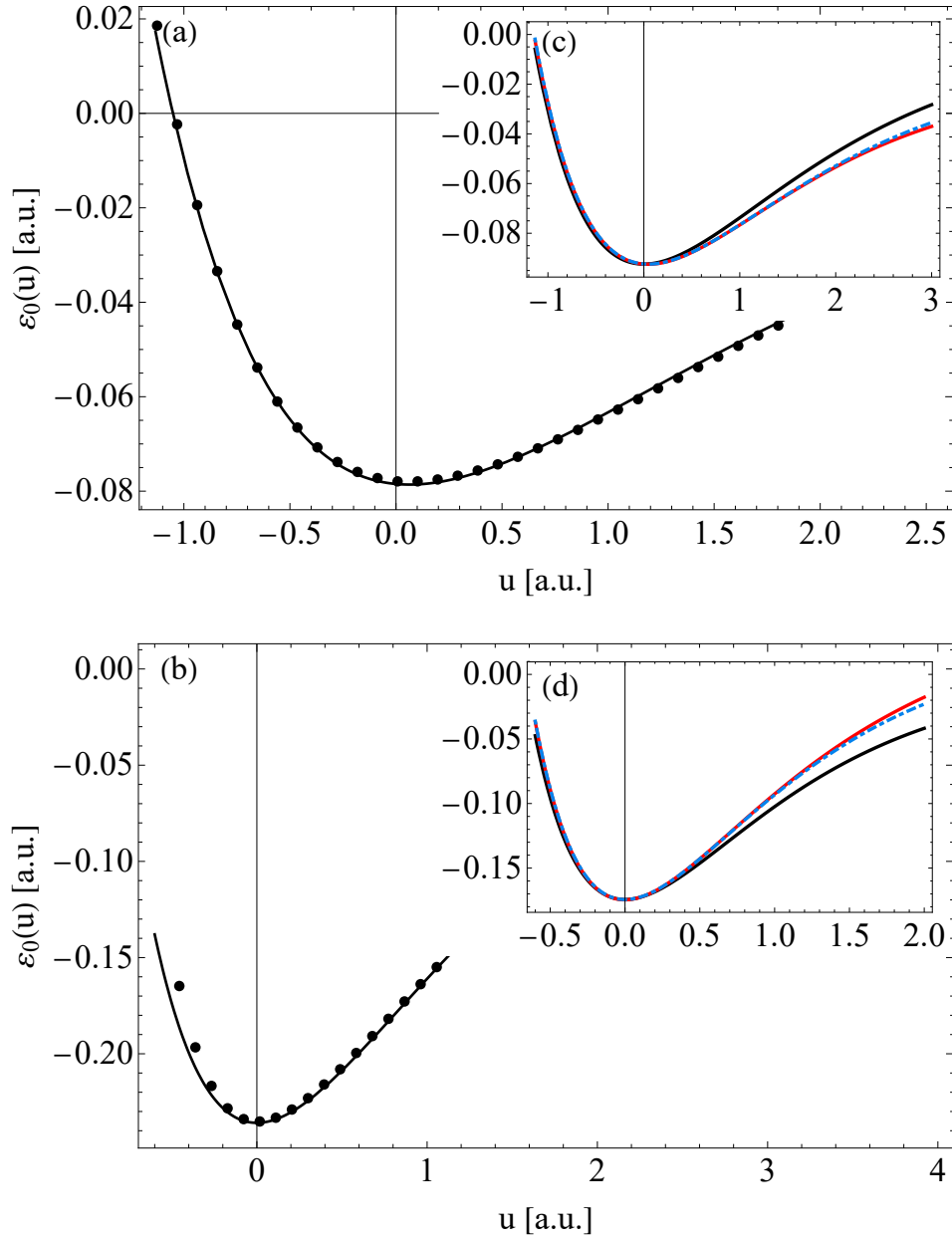


Figure 1. Potential energy curves of LiH (upper panel) and H₂ (lower panel) according to different models. On (a) and (b) the dots give the values of $\varepsilon_0(u, 0)$ computed by DFT in the indicated range of internuclear separation (u), and the solid line plots the Morse potential $V_M(u)$ fitted to the computed values. The insets (c) and (d) show $V_M(u)$ (black solid line), the term $V_M(u) - \frac{\alpha_1 F_0^2}{4} u$ from (10) (red solid line) and the analytically fitted Morse potential $\mathcal{V}_M(u)$ (blue dash-dotted line) according to (11) for $F_0 = 0.02$ a.u..

In the case of H_2 , since it is a homonuclear molecule, μ_0 and μ_1 disappear in (6), and α_0 and α_1 are the leading and thus the significant terms. Furthermore, figure 1 (c) and (d) clearly show that the $V_M(u) - \frac{\alpha_1 F_0^2}{4}u$ term in (8) is really well approachable by Morse potential having different parameters than the original one of the given molecule. However, the polarizability gradient has a different sign for these two molecules. For LiH the polarizability gradient has a positive sign, thus $V_M(u) - \frac{\alpha_1 F_0^2}{4}u$ appears as a less bonding potential. While the polarizability gradient of H_2 has a negative sign, therefore $V_M(u) - \frac{\alpha_1 F_0^2}{4}u$ describe a more bonding potential. The above statements are also supported by the difference of the number of bound states between the original Morse potential, $V_M(u)$, and the approximated potential, $\bar{V}_M(u)$. For a Morse potential with given parameters the number of bonding states is the integer part of the following:

$$N(D, a, M_n) = \frac{2D - \hbar\omega_0}{\hbar\omega_0}, \quad (20)$$

where ω_0 depends on the parameters of the Morse potential as stated above. In the absence and presence of a laser field having 0.02 a.u. field strength and 1500 nm wavelength, LiH has 27 and 25 bound states, while for H_2 these numbers are 16 and 18, respectively.

Figure 3 shows how a laser field having the indicated parameters distorts the potential energy curves of LiH (a) and of H_2 (b). The first seven energy levels belonging to $V_M(u)$ and $\bar{V}_M(u)$ are also indicated on figure 3 and they clearly show how the laser field shifts the vibrational levels of the molecules. For LiH, as $\bar{V}_M(u)$ is less bonding potential than $V_M(u)$, the spacing between the energy levels are smaller in the presence of the laser field. In the case of H_2 , the opposite is true, the distances between the energy levels are larger than the originals due to the fact that $\bar{V}_M(u)$ is more bonding potential than $V_M(u)$.

In order to further investigate the applicability of our method we examine how the spacing of the shifted energy levels varies with the laser wavelength. The relative shift of the transition energy levels of $\bar{V}_M(u)$ compared to the energy level spacing of $V_M(u)$ is the following:

$$\Delta_n = \frac{|\Delta E_n - \Delta \mathcal{E}_n|}{\Delta E_n}, \quad (21)$$

where $\Delta E_n = E_n - E_{n-1}$ and $\mathcal{E}_n = \mathcal{E}_n - \mathcal{E}_{n-1}$ are the differences of the energy eigenvalues of $V_M(u)$ and of $\bar{V}_M(u)$, respectively. The (21) quantity in atomic units is actually identical to the relative shifts of vibrational transition frequency. We present the wavelength dependence of Δ_n for the first six vibration transition for both molecules on figure 4. The shift of the transition energy values caused by the laser field is approximately independent of laser wavelength. This suggests that our model can also be applied to laser pulses in the IR spectral range.

5. Summary

We derived analytic expressions, (18) and (19), which are valid in a wide wavelength range to account for the effect of a strong long laser pulse on the vibrational levels and the bond-length change of a diatomic molecule with high accuracy. These results can be readily applied both to heteronuclear and to homonuclear diatomic molecules and to certain (e.g. alkali metal) atomic dimers. Our model can be relevant also in cases where the Morse potential can be used to describe certain interactions, like weakly bound hydrogen in a larger molecule [59, 60], polyatomic molecule with a single weak internal bond, and the interaction of an atom or a diatomic molecule with a solid surface [61, 62]. The resulting level shifts and the corresponding vibrational transition frequency shifts can be readily measured with state of the art spectroscopic methods, both in laboratory and in astrophysical observations.

6. Acknowledgment

We thank F. Bogár and Á. Vibók for stimulating discussions. The ELI ALPS project (GINOP-2.3.6-15-2015-00001) is supported by the European Union and co-financed by the European Regional Development Fund. One of the authors (G.P.) acknowledges the financial support from the Hungarian Government under project number 2018-1.2.1-NKP-2018-00010.

References

- [1] Palacios A, Sanz-Vicario J L and Martín F 2015 *Journal of Physics B: Atomic, Molecular and Optical Physics* **48** 242001
- [2] Halász G J, Vibók A and Cederbaum L S 2015 *The Journal of Physical Chemistry Letters* **6** 348–354
- [3] Nisoli M, Decleva P, Calegari F, Palacios A and Martín F 2017 *Chemical Reviews* **117** 10760–10825
- [4] Carrera J J, Tong X M and Chu S I 2006 *Physical Review A* **74** 023404
- [5] Goulielmakis E, Schultze M, Hofstetter M, Yakovlev V S, Gagnon J, Uiberacker M, Aquila A L, Gullikson E M, Attwood D T, Kienberger R, Krausz F and Kleineberg U 2008 *Science* **320** 1614–1617
- [6] Chini M, Zhao K and Chang Z 2014 *Nature Photon* **8** 178
- [7] Gaumnitz T, Jain A, Pertot Y, Huppert M, Jordan I, Ardana-Lamas F and Wörner H J 2017 *Optics Express* **25** 27506–27518
- [8] Krausz F and Ivanov M 2009 *Reviews of Modern Physics* **81** 163–234
- [9] Itatani J, Quéré F, Yudin G L, Ivanov M Y, Krausz F and Corkum P B 2002 *Physical Review Letters* **88** 173903
- [10] Kitzler M, Milosevic N, Scrinzi A, Krausz F and Brabec T 2002 *Physical Review Letters* **88** 173904
- [11] Eckle P, Smolarski M, Schlup P, Biegert J, Staudte A, Schöffler M, Müller H G, Dörner R and Keller U 2008 *Nature Physics* **4** 565–570
- [12] Wei M, Quan W, Sun R, Xu S, Xiao Z, Zhou Y, Zhao M, Hao X, Duan C and Liu X 2018 *Physical Review A* **98** 063418
- [13] Wang F, Liu K, Zhang X, Wang Z, Qin M, Liao Q and Lu P 2019 *Phys. Rev. A* **100** 043405
- [14] Biswas S, Förg B, Ortman L, Schötz J, Schweinberger W, Zimmermann T, Pi L, Baykusheva

- D, Masood H A, Lontos I, Kamal A M, Kling N G, Alharbi A F, Alharbi M, Azzeer A M, Hartmann G, Wörner H J, Landsman A S and Kling M F 2020 *Nature Physics* **16** 778–783
- [15] URL <https://tomatto.eu/p1-new-attosecond-beamline/>
- [16] Friedrich B and Herschbach D 1995 *Physical Review Letters* **74** 4623–4626
- [17] Simkó I, Chordiya K, Császár A G, Kahaly M U and Szidarovszky T 2022 *Journal of Computational Chemistry* **43** 519–538
- [18] Seideman T 1995 *The Journal of Chemical Physics* **102** 6487–6498
- [19] Kapteyn H C, Murnane M M, Szoke A and Falcone R W 1991 *Optics Letters* **16** 490–492
- [20] Varró S 2022 *New Journal of Physics* **24** 053035
- [21] Bandrauk A D 1994 *Molecules in Laser Field* (Marcel Dekker, Inc.)
- [22] Šindelka M and Moiseyev N 2006 *The Journal of Physical Chemistry A* **110** 5561–5571
- [23] Majorosi S and Czirják A 2016 *Computer Physics Communications* **208** 9–28
- [24] Majorosi S, Benedict M G and Czirják A 2018 *Physical Review A* **98** 023401
- [25] Majorosi S, Benedict M G, Bogár F, Paragi G and Czirják A 2020 *Physical Review A* **101** 023405
- [26] Morse P M 1929 *Physical Review* **34** 57–64
- [27] Ter Haar D 1946 *Physical Review* **70** 222–223
- [28] Varshni Y P 1957 *Reviews of Modern Physics* **29** 664–682
- [29] Tietz T 1963 *Journal of Chemical Physics* **38** 3036
- [30] Hua W 1990 *Physical Review* **42** 2524–2529
- [31] Benedict M G and Molnár B 1999 *Physical Review A* **60** R1737–R1740
- [32] Molnár B, Földi P, Benedict M G and Bartha F 2003 *Europhysics Letters* **61** 445–451
- [33] Földi P, Benedict M, Czirják A and Molnár B 2003 *Physical Review A* **67** 0321104
- [34] Chu S 1981 *The Journal of Chemical Physics* **75** 2215–2221
- [35] Ting J J L 1994 *Journal of Physics B: Atomic, Molecular and Optical Physics* **27** 1249
- [36] Yuan J M and Liu W K 1998 *Physical Review A* **57** 1992–2001
- [37] Murphy D S, McKenna J, Calvert C R, Williams I D and McCann J F 2007 *New Journal of Physics* **9** 260
- [38] Triana J F and Herrera F 2022 *New Journal of Physics* **24** 023008
- [39] Gready J E, Bacskay G and Hush N 1977 *Chemical Physics* **22** 141–150
- [40] Gready J E, Bacskay G and Hush N 1977 *Chemical Physics* **23** 9–22
- [41] Gready J E, Bacskay G and Hush N 1977 *Chemical Physics* **24** 333–341
- [42] Born M and Oppenheimer R 1927 *Annalen der Physik* **389** 457–484
- [43] Kramers H A 1956 *Collected Scientific Papers* (North-Holland: Amsterdam)
- [44] Henneberger W C 1968 *Physical Review Letters* **21** 838–841
- [45] Varró S and Ehlötzky F 1993 *Nouvo Cimento* **15 D** 1371–1396
- [46] Varró S, Földi P and Barna I F 2019 *Journal of Physics: Conference Series* **1206** 012005
- [47] Shi, Y B, Stancil, P C and Wang, J G 2013 *Astronomy & Astrophysics* **551** A140
- [48] Kang X, Fang Z, Kong L, Cheng H, Yao X, Lu G and Wang P 2008 *Advanced Materials* **20** 2756–2759
- [49] Bougleux E and Galli D 1997 *Monthly Notices of the Royal Astronomical Society* **288** 638–648
- [50] Bovino S, Čurík R, Galli D, Tacconi M and Gianturco F A 2012 *The Astrophysical Journal* **752** 19
- [51] Wang Y and Ma J 2009 *Journal of Organometallic Chemistry* **694** 2567–2575
- [52] Ibrahim H, Lefebvre C, Bandrauk A D, Staudte A and Légaré F 2018 *Journal of Physics B: Atomic, Molecular and Optical Physics* **51** 042002
- [53] Frisch M J, Trucks G W, Schlegel H B, Scuseria G E, Robb M A, Cheeseman J R, Scalmani G, Barone V, Petersson G A, Nakatsuji H, Li X, Caricato M, Marenich A V, Bloino J, Janesko B G, Gomperts R, Mennucci B, Hratchian H P, Ortiz J V, Izmaylov A F, Sonnenberg J L, Williams-Young D, Ding F, Lipparini F, Egidi F, Goings J, Peng B, Petrone A, Henderson T, Ranasinghe D, Zakrzewski V G, Gao J, Rega N, Zheng G, Liang W, Hada M, Ehara M, Toyota K, Fukuda R, Hasegawa J, Ishida M, Nakajima T, Honda Y, Kitao O, Nakai H, Vreven T, Throssell K,

Montgomery Jr J A, Peralta J E, Ogliaro F, Bearpark M J, Heyd J J, Brothers E N, Kudin K N, Staroverov V N, Keith T A, Kobayashi R, Normand J, Raghavachari K, Rendell A P, Burant J C, Iyengar S S, Tomasi J, Cossi M, Millam J M, Klene M, Adamo C, Cammi R, Ochterski J W, Martin R L, Morokuma K, Farkas O, Foresman J B and Fox D J 2016 Gaussian~16 Revision B.01 gaussian Inc. Wallingford CT

- [54] Zapata J C and McKemmish L K 2020 *The Journal of Physical Chemistry A* **124** 7538–7548
- [55] Hait D and Head-Gordon M 2018 *Journal of Chemical Theory and Computation* **14** 1969–1981
- [56] Becke A D 1993 *The Journal of Chemical Physics* **98** 5648–5652
- [57] Weigend F and Ahlrichs R 2005 *Physical Chemistry Chemical Physics* **7** 3297–3305
- [58] Weigend F 2006 *Physical Chemistry Chemical Physics* **8** 1057–1065
- [59] Blaise P and Henri-Rousseau O 2000 *Chemical Physics* **256** 85–106
- [60] Zdravković S and Satarić M V 2006 *Physical Review E* **73** 021905
- [61] Galashev A Y, Katin K P and Maslov M M 2019 *Physics Letters A* **383** 252–258
- [62] Safina L R, Baimova J A and Mulyukov R R 2019 *Mechanics of Advanced Materials and Modern Processes* **5** 2

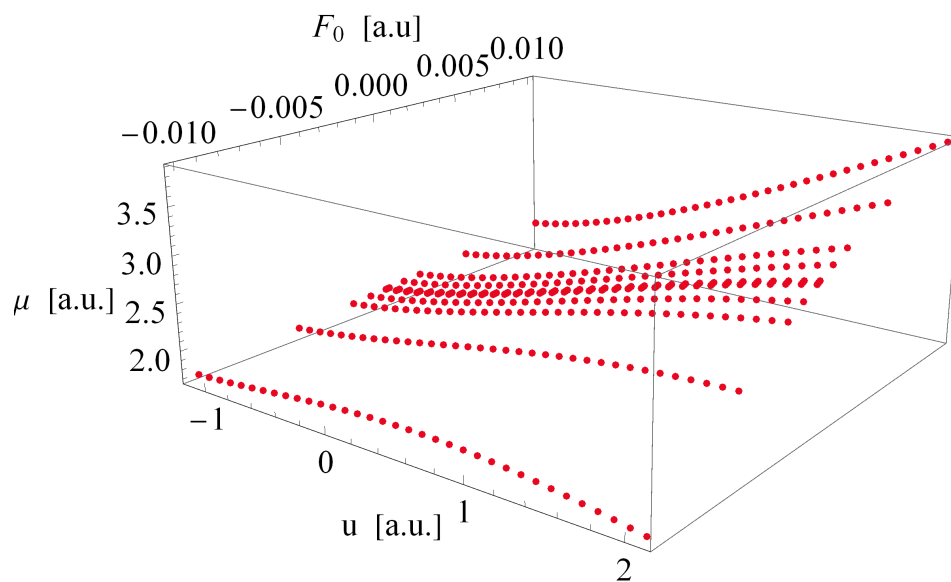


Figure 2. Field-dependent dipole moment values ($\mu(u, F(t))$) of LiH computed by DFT in the indicated range of internuclear separation (u) and of static electric field strength (F_0).

Table 1. The numerical values in a.u. of the parameters of the dipole moment function, (6) and of the field-free and the shifted Morse potential for both LiH and H₂. The parameters of the laser field are $F_0 = 0.02$ a.u. and $\lambda = 1500$ nm.

	μ_0	μ_1	α_0	α_1	D	a	R_0	\bar{D}	\tilde{a}	\bar{R}_0
LiH	2.261	0.3673	35.72	29.16	0.09242	0.5969	3.016	0.08194	0.6078	3.064
H ₂	0	-54.98	0	-128.9	0.1744	1.028	1.401	0.2019	1.005	1.368

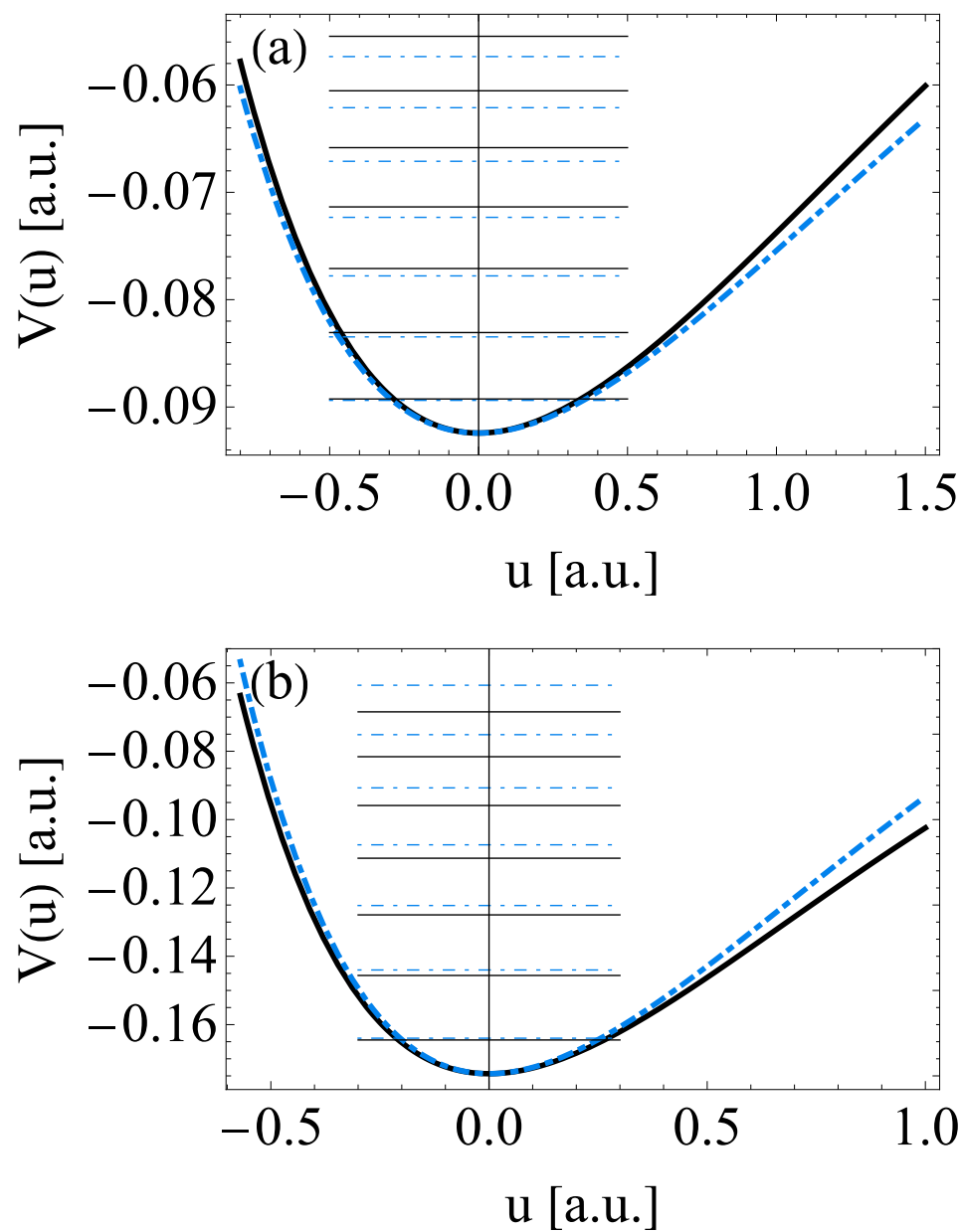


Figure 3. The field-free ($V_M(u)$) and the shifted Morse potential ($\bar{V}_M(u)$) of LiH (a) and H_2 (b) plotted by black solid curve and blue dash-dotted curve, respectively. The horizontal lines with corresponding styles mark the first seven energy levels of the corresponding Morse potential. The parameters of the laser field are $F_0 = 0.02$ a.u. and $\lambda = 1500$ nm.

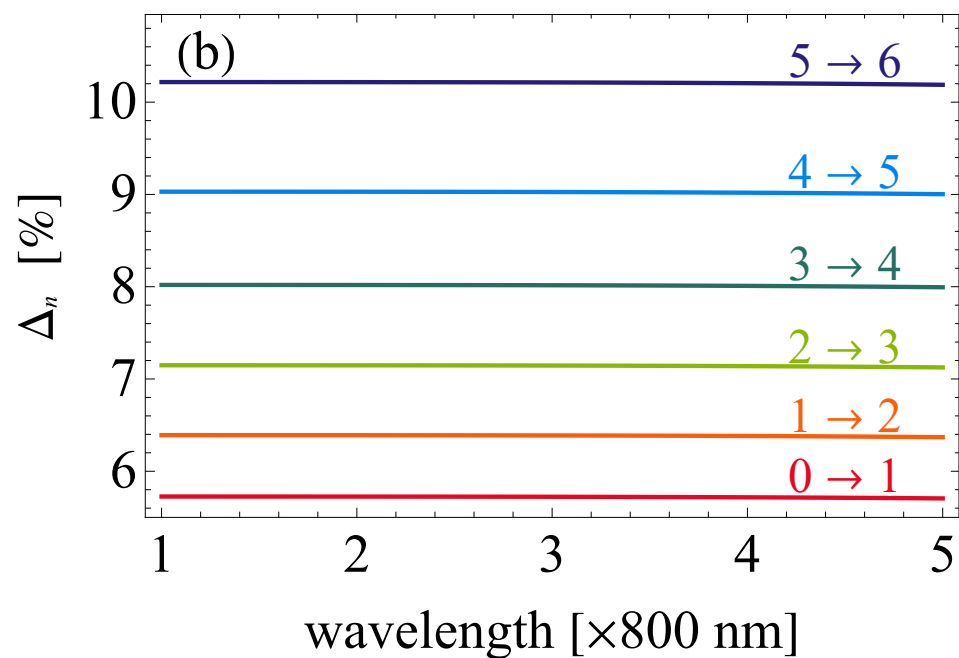
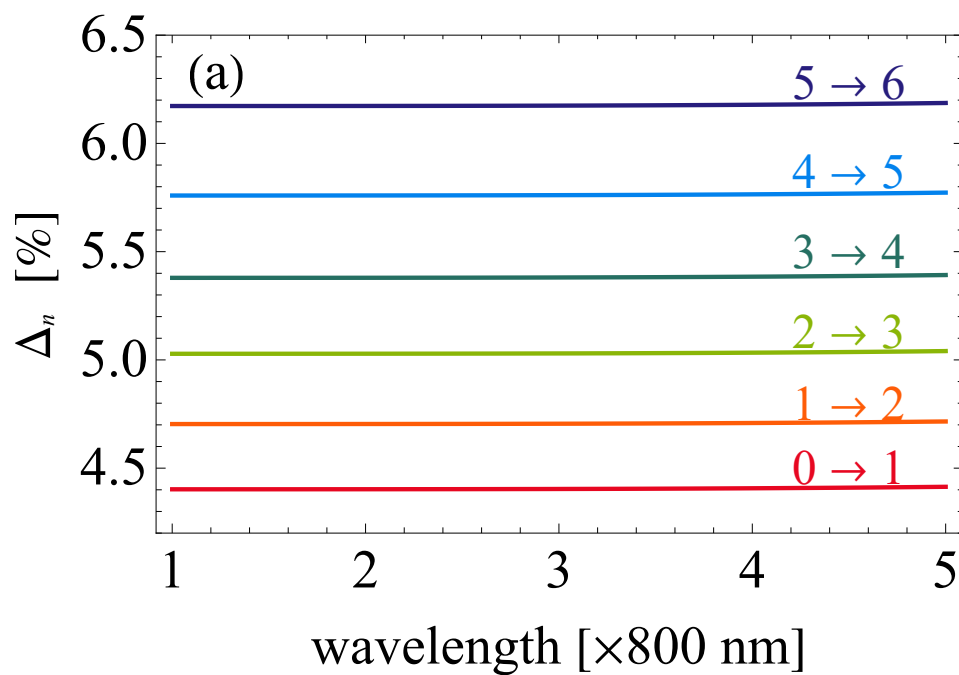


Figure 4. Relative shifts of vibrational transition frequency caused by the laser field for the first six energy levels for LiH (a) and for H₂ (b) as a function of laser wavelength in case of $F_0 = 0.02$ a.u..